On the Feasibility of Hybrid Battery/Ultracapacitor Energy Storage Systems for Next Generation Shipboard Power Systems

Yichao Tang, *Student Member, IEEE*, and Alireza Khaligh, *Senior Member, IEEE*
Energy Harvesting and Renewable Energies Laboratory (EHREL),
Department of Electrical and Computer Engineering,
Illinois Institute of Technology, Chicago, IL 60616, Phone: +1 (312) 567-3444, Fax: +1 (312) 567-8976
EML: ytang5@iit.edu, khaligh@ece.iit.edu, URL: www.ece.iit.edu/~khaligh

***Abstract* – This paper explores a Battery/Ultracapacitor Energy Storage System (BUCESS) for navy application. A new configuration of the battery and ultracapacitor combined system is introduced for propulsion system and pulse power loads. A dual active bridge (DAB) topology is selected to control the bidirectional power flow through phase shifting for charging and discharging batteries and ultracapacitors. High-frequency switching devices are selected to achieve dc-dc conversion at high voltage and high power levels. A 500V-1kV BUCESS is designed and analyzed to investigate 100kW transmission for batteries and 1MW for ultracapacitors both in charging and discharging modes.**

Keywords – battery, dual active bridge, energy storage system, navy, phase-shift soft switching, ship, ultracapacitor.

I. INTRODUCTION

Batteries, ultracapacitors (UC), superconducting magnetic energy storage (SMES), and flywheels are candidates for energy storage systems (ESS) of next generation shipboard power systems. Batteries have the highest energy densities among these technologies, which is almost ten times that of other devices, though the power densities of batteries are less than $1/10^{th}$ that of other technologies. Therefore, the runtime of batteries can reach from 5 minutes to 8 hours that makes batteries suitable candidates as primary long-term and median-term source of backup power, while ultracapactiors, flywheels, and SMES can only run within 1 minute and are usually pertinent candidates as short-term sources to supply pulse power loads [1]. Fig. 1 shows the classification of batteries, UCs and flywheels based on their energy density and power density. The runtime of batteries is far more than those of other technologies. UCs and flywheels have significantly faster response in providing power to the load than batteries, while UCs show better characteristics than flywheel both in energy density and power density.

Batteries have been employed in most navy ships as standby storage devices to support loads until an alternative source such as a diesel generator is available. Flywheel systems have been widely researched and can be a replacement for batteries in some specific situations, where only short runtimes are needed. In other cases such as navy application which needs long runtimes, flywheels are usually in conjunction with batteries so that the ESS can perform well in both short time and long time. By contrast, batteries and UCs conjunction systems applied in shipboard power system have not been extensively explored, though such systems are broadly being examined for future land vehicles and trucks.

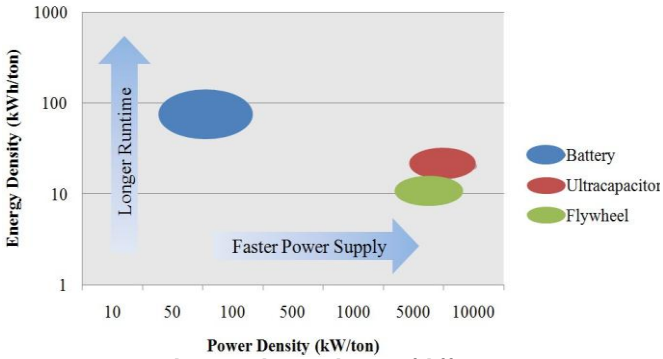

Fig. 1. Energy density and power density of different energy storage technologies

UCs have superiorities in many aspects beyond flywheels, such as lower standby losses of full load rating, higher power density, instantaneous recharge, higher stability and safety, some of which, such as the lower standby losses 0.2% of UCs compared to 2% of flywheels, are significantly important in naval application. For naval applications which are usually multiple megawatts, supporting a 4MW propulsion motor through inefficient flywheel system over the 10-year lifetime, will consume approximately 350 million kWh, equivalent to $35 million. Then the extra 1.8 percentage standby losses of flywheel systems will lead to an extra $630,000 compared to UC systems.

II. POWER REQUIREMENTS

Determining the power range of the ship loads is required in order to design the battery/ultracapacitor energy storage system and its power electronic interfaces. The power of propulsion system strongly depends on the speed of ships which may be varied in a period of time. Fig. 2 shows the detailed speed changes for the USS *Arleigh Burke* (DDG-51)'s one day operation, based on its average operation in June 1998 measured by Naval Archives [2]. The speeds of the naval ship are distributed in the range of 5~27 knots, where low speed is within 15kns and high speed reaches over 25kns. The significant amount of operation time in practice is from 5kns to 20kns, which means low and mediate speed operations are significantly important and frequent. The operation time at low speed has a high proportion at 70% of the total period compared to only 5% of high speed operation.

The speed distribution seems having no regular pattern. During the 17^{th} day and 18^{th} day, the speed variation happens more frequently in some periods such as 5:00~9:00 a.m., 1:00~5:00 p.m. and 7:00~9:00 p.m. The ship operates at the

978-1-4244-8218-4/10/$26.00 ©2010 IEEE

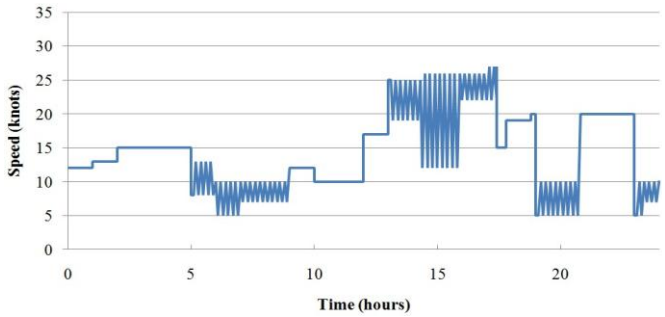

Fig. 2. Speed distribution of DDG51 within one day at the beginning of 6-month deployment

low speed areas such as harbors, while the ship operates at high speeds in the sea, in period of 1:00~5:00 p.m..

The relationship between speed and output power is nonlinear [3]. A ship to be driven up to 25kns needs a 70MW main engine, but if the speed is reduced to 20 knots only 36MW power is required. Continuous slowing down the speed to 12kns will reduce the power demand to lower than 8MW. As an example, the Dutch navy's *Zeven Provinciën class of guided-missile destroyers* [4], which is a 144m ship has two 5MW diesel engines and two 20MW gas turbines. With two diesel generators and one gas turbine, which would lead to 30MW total available generation, the ship can keep the speed at 25.5kns. Combining this system with a 14MWh battery, the ship can attain its top speed at 28kns for additional 1 hour.

Based on the nonlinear relationship between speed and output power, the power distribution of DDG51's within one day is plotted in Fig. 3. During the periods of 1:00~5:00 p.m., the average power is approximately 25MW and varies not only frequently but also significantly, which needs frequent shift of UCs between charging and discharging modes.

From Fig. 3 the output power for propulsion system should be about 3MW at low speed and 40MW at high speed. At low speed, the ESS should support the propulsion system independently for 3~4 hours. If the ship is equipped with two 5MW diesel engines and one 15MW gas turbine for propulsion system at high speed, extra 15MW is still needed from the ESS for 20~30 seconds. Besides, pulse power loads like weapon system also demand 30MW for 10~20 seconds. Therefore, if the whole storage system consists of 30 BUCESS units, a single unit is demanded to supply 100kW

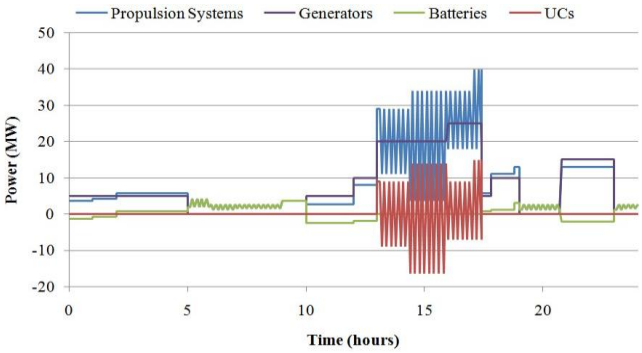

Fig. 3. Output power of propulsion systems, generators, batteries and UCs in period of one day

power by batteries for low speed propulsion, 500kW by UCs for high speed propulsion and 1MW by UCs for pulse power loads.

III. TOPOLOGY AND OPERATION OF BUCESS

Battery/ultracapacitor combined system is being explored for land hybrid electric vehicles (HEVs) [6]. A typical BUCESS topology is provided in Fig. 4, where the battery is directly connected to dc bus and only a bidirectional dc-dc converter controls power flow. Although the configuration and control is simple, the voltage of battery has to be close to dc bus voltage and the flexibility of controlling battery power is limited. The stability issues such as inrush current can damage the UC when charged directly from dc bus without any protection. Since BUCESS for navy ship has to meet the requirements of high voltage and high power charging and discharging, a more flexible and stable system is demanded.

The dc zonal distribution system of a navy ship has two kinds of dc voltage level: one is high voltage level (between 4.7kV and 10kV) and the other is medium voltage level (between 700V and 1kV) [7]. The high voltage dc bus which is called main dc bus is directly connected by generators, propulsion motors and pulse power loads while the medium one called zone dc bus is mainly for critical loads like energy storage system. The BUCESS has to be connected to 1kV dc bus.

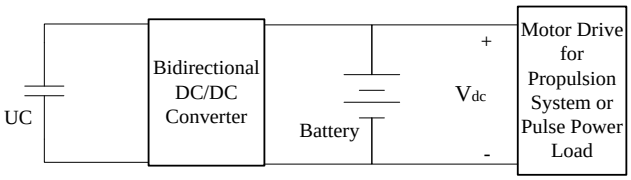

Fig. 4. Typical BUCESS topology for land HEVs

The new configuration of BUCESS for navy application is demonstrated in Fig. 5. The bidirectional dc-dc converter I between batteries and dc bus, and the bidirectional converter III between batteries and UCs are mainly used to transfer 100kW power. When electro-mechanic switch K1 is ON, K2 is OFF, the system operates in battery discharging mode. When K1 is OFF, the batteries are charged by dc bus. Since the UCs primarily supply extremely high power for high speed propulsion and pulse power loads, when K3 is ON, the bidirectional dc-dc converter II is utilized for 1MW charging (K2 is ON) and discharging (K2 is OFF) of UCs. The batteries and the UCs are also capable of being combined discharged via converter I and II. The advantages of employing two dc-dc converters for batteries and UCs respectively can be concluded as: (1) flexibility of designing converters for different power conversion levels (battery for 100kW & UC for 1MW), (2) lower stress for each converter leading to longer lifetime and lower maintenance cost, (3) better isolation between batteries and UCs, (4) continuous power supply when one converter is damaged.

Batteries can also charge UCs through the bidirectional converter III. If the upper limit voltage of UCs is set to be

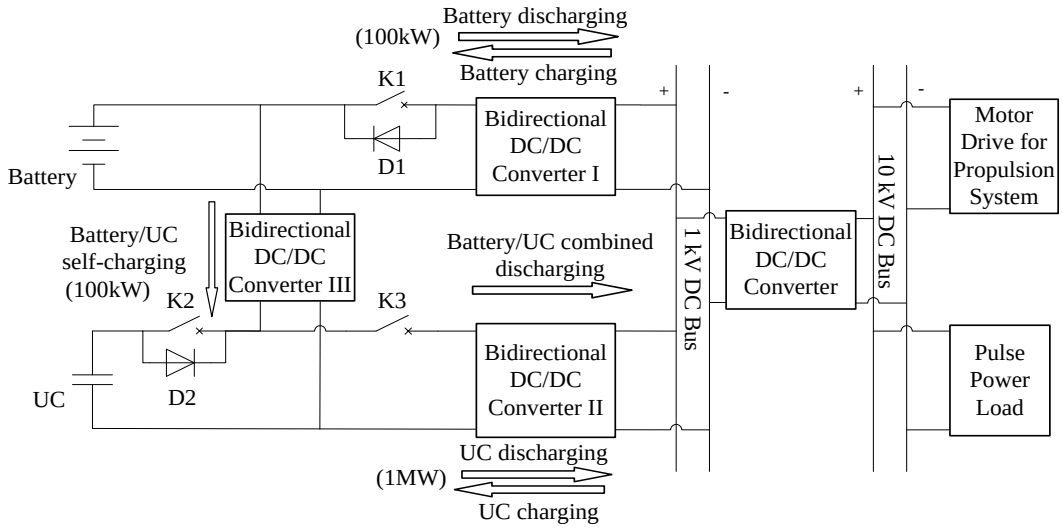

Fig. 5. New BUCESS topology for naval applications

equal to that of batteries, as the UCs are charged to 80% of full energy capacity by 1MW power from dc bus, the voltage of UCs increases to 90% of batteries voltage. K3 is turned OFF and K2 keeps ON, the dc-dc converter III works in buck mode and batteries can slowly charge UCs at 100kW. When UCs are fully charged and K2 is turned OFF, UCs can supply power to batteries via D2, which plays a key role in protecting UCs from overcharge.

The battery module is composed of 12 parallel lithium-ion battery strings, each of which consists of 20 25.2V/58Ah modules. Therefore, the voltage of battery module can reach 500V that can be easily boosted to 1kV and the energy capacity is about 350kWh. The UC module consists of 14 parallel UC strings, each of which has four 125V/101.7Wh/18.75kW/63F UC modules in series. If the output power keeps constant at 1MW,

$$P = I_c U_c = C\frac{du_c}{dt}U_c \Rightarrow PT = C\int_{V_1}^{V_2} U_c du_c$$

the voltage of UC module can drop from the rated voltage of 500V to 67% of the rated voltage within 15 seconds, which means the UCs are discharged to 44% of full energy capacity. If 30 such combined battery/UC modules are used as energy storage system, the battery modules can individually support 3MW (each for 100kW) to the propulsion motors for 3.5 hours during low speed operation and the UC modules are capable of providing 15MW (each for 500kW) for 30 seconds during high speed operation. Moreover, the UC modules can offer 30MW (each for 1MW) to weapon systems for about 15 seconds.

IV. HIGH-POWER BIDIRECTIONAL DC-DC CONVERTER

Since the power flow via the dc-dc converters between battery/UC systems and dc bus is significantly large, isolated transformers are demanded to protect the ESS and the whole power system from unexpected damages, such as module fault or power down. Among several dc-dc converters with transformers such as flyback, forward, pull-push, half-bridge and full-bridge, the full-bridge dc-dc converter is most suitable for high voltage and high power applications. This is due to the fact that lower stress and large transformer core can be obtained in this topology. Although half-bridge dc-dc converter is an alternative for half as many active devices as the full-bridge, the later has lower stress in devices and is more suitable for high-voltage input.

Various full bridge dc/dc converters for high power applications, including series/parallel resonant (SPR), phase-shifted bridge, hard-switched PWM and dual active bridge (DAB), are discussed in [9]. Among these topologies, the dual active bridge is considered an excellent alternative for bidirectional high power flow applications such as battery charge/discharge operation. The DAB has a high-frequency transformer and two voltage-sourced active bridges at primary and secondary sides, each with four switches operating at constant frequency. The topology needs no output inductor and the resonant inductance has been built into the transformer. Each bridge can generate a high-frequency square wave voltage at the transformer terminal and the power flow from one dc source to another can be controlled by phase-shifting the two square waves. The converter can also boost and buck voltage and transfer bidirectional power. The DAB showed in Fig. 6 uses eight IGBTs specifically designed for 100kW charging and

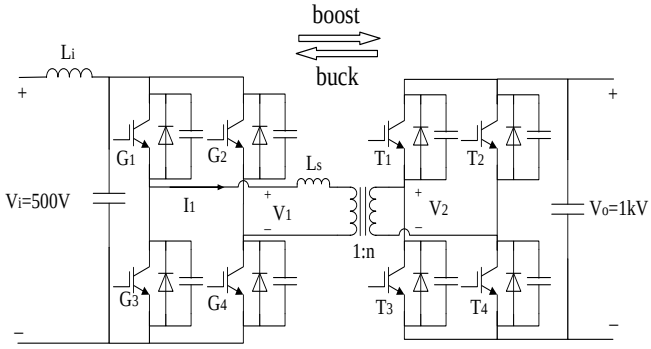

Fig. 6. Dual active full bridge dc-dc converter for 100kW

discharging of batteries.

Even though the bidirectional dc-dc converter II is needed for 1MW charging and discharging of UCs, the DAB is also a suitable candidate due to soft switching, low devices stress, and less components. Since the average current at low voltage side can reach more than 2000A due to extremely high power flow, IGBTs are not excellent choices for 1MW converter. Table I provides the capabilities of different switching devices, where GTO is the best alternative for 1MW application. Despite the low frequency operation capability (3kHz) of GTO, this is not a serious problem as higher switching frequency causes significantly high losses both in switches and transformers at 1MW level. In addition, according to Table I, IGBT is suitable for 100kW dc-dc conversion if the peak current at low voltage side is limited to 400A.

TABLE I
CAPABILITIES OF DIFFERENT SWITCHING DEVICES

Type of switches	Frequency(kHz)	Voltage(kV)	Current(A)
Thyristors	0.5	5	3000
GTOs	3	6	6000
IGBTs	80	3.3	1400
MCTs	30	0.6	600
BJTs	10	1.2	800
MOSFETs	100	1	50

V. PHASE-SHIFT SOFT SWITCHING

The DAB converter in Fig. 6 is controlled by phase-shift soft switching, where V_1 is the voltage of primary side, V_2 is the voltage of secondary side, and L_s is the leakage inductor. If the leakage resistance and the magnetic impedance are neglected, the primary referenced equivalent circuit can be achieved by replacing the transformer with the leakage inductor. Fig. 7 demonstrates the four operation modes of the DAB in one switching period. When G_1 and G_4 are ON, G_2 and G_3 are OFF, $V_1 = V_i$; when G_2 and G_3 are ON, G_1 and G_4 are OFF, $V_1 = -V_i$; when T_1 and T_4 are ON, T_2 and T_3 are OFF, $V_2 = V_o$; when T_2 and T_3 are ON, T_1 and T_4 are OFF, $V_2 = -V_o$. In one switching period, if the duty cycles, *D*, of both sides are equal to 0.5 and the phase of square wave of secondary side is shifted by αT, the current waveform of primary side can be obtained as shown in Fig. 8.

When $0 < t < \alpha T$,

$$I(\alpha T) - I(0) = \frac{V_i - (-V_o)}{L_s}\alpha T \tag{1}$$

When $\alpha T < t < 0.5T$,

$$I(0.5T) - I(\alpha T) = \frac{V_i - V_o}{L_s}(0.5-\alpha)T \tag{2}$$

Since the average value of primary side current is equal to zero, it is not difficult to find the symmetrical relationship that $I(0.5T) = -I(0)$ and $I((0.5+\alpha)T) = -I(\alpha T)$. Then the current value at zero point and shifting point can be calculated by equations (3) and (4).

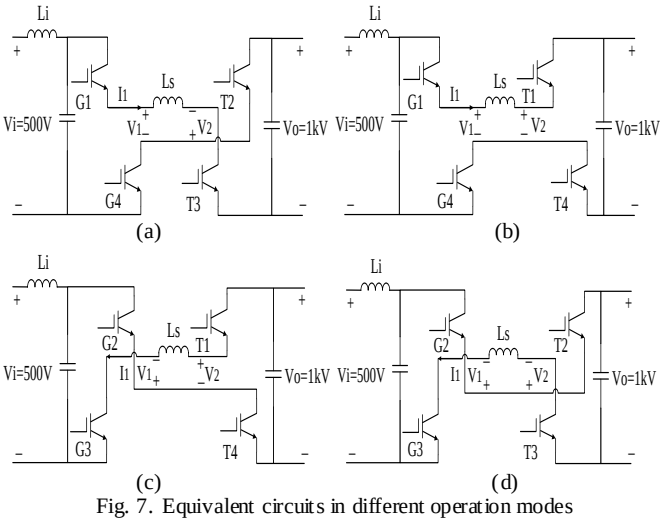

Fig. 7. Equivalent circuits in different operation modes

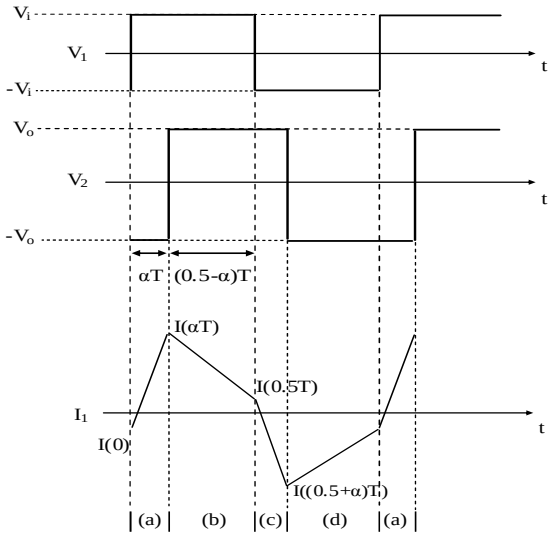

Fig. 8. Ideal voltage waveforms of primary side and secondary side & ideal current waveform of primary side in one switching period

$$I(0) = \frac{\frac{1}{4}(V_o - V_i) - \alpha V_o}{L_s}T \tag{3}$$

$$I(\alpha T) = \frac{\frac{1}{4}(V_o - V_i) + \alpha V_i}{L_s}T \tag{4}$$

Assuming steady state operation $\frac{V_o}{V_i} = \frac{I_1}{I_2} = n$, the output power of the circuit can be calculated as:

$$P_o = \frac{\int_0^T V_2 I_2 dt}{T} = \frac{2\int_{\alpha T}^{(0.5+\alpha)T} V_o I_2 dt}{T} = \frac{2V_i \int_{\alpha T}^{(0.5+\alpha)T} I_1 dt}{T} \tag{5}$$

By calculating the area of primary current from αT to (0.5+α)T in Fig. 8, the output power becomes

$$P_o = \frac{V_i^2}{L_s f}\alpha(1-2\alpha) \tag{6}$$

When $0<\alpha<0.5$, the output power is positive, indicating that the converter is operating in discharging mode; when

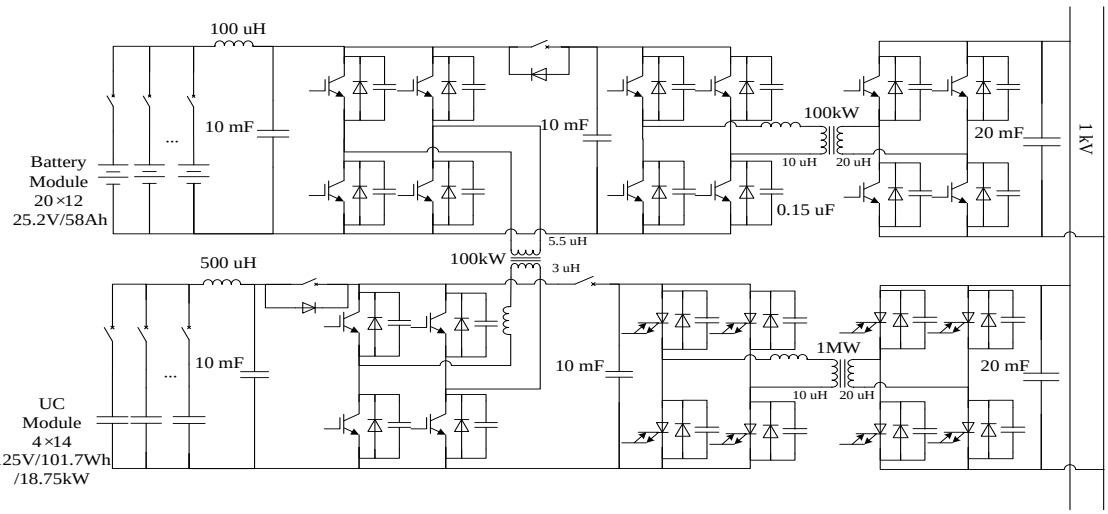

Fig. 9. Detailed BUCESS topology.

0.5<α<1, the output power is negative demonstrating that the converter is working in charging mode.

And the shifted phase can be calculated as:

$$\alpha^2 - 0.5\alpha + \frac{P_o L_s f}{V_i^2} = 0 \Rightarrow \alpha = \frac{0.5 \pm \sqrt{0.25 - \frac{2P_o L_s f}{V_i^2}}}{2} \quad (7)$$

when α = 0.25,

$$P_{\max} = \frac{V_i^2}{8L_s f} \Rightarrow L_s \le \frac{V_i^2}{8P_{\max} f} \quad (8)$$

As the switching frequency for UC module is 1kHz at 1MW, the leakage inductor L_s would be 31μH. A 15μH leakage inductor is chosen to minimize the inductor losses.

The switching frequency of the 100kW dc-dc converter is chosen 10kHz. The leakage inductor L_s would be 15μH between batteries and dc bus, and 10μH between batteries and UCs. Other parameters of BUCESS are demonstrated in TABLE II.

VI. Simulation Results

Fig. 9 shows the analyzed BUCESS topology. The block diagram of phase-shifted soft switching is shown in Fig. 10.

The simulation results from Fig. 11 to Fig. 17 show power flow among batteries, UCs and dc bus from full loads to 50% of full loads for different operation modes.

The dc bus voltage can keep at 1kV when the loads or sources have step changes. The output power is stable when batteries and UCs are discharged half of the energy capacity, and the efficiencies of each mode are beyond 90%. The results demonstrate that the system is feasible and stable for different power requirements.

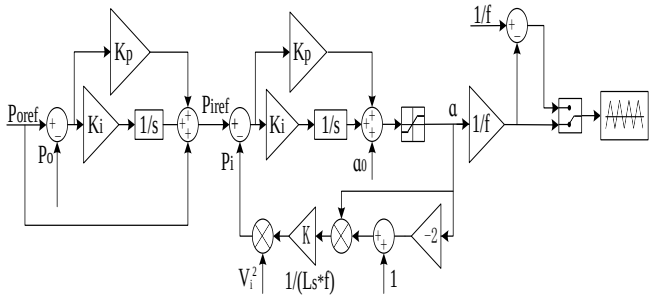

Fig. 10. Block diagram of phase-shift soft switching

TABLE II
PARAMETERS OF BUCESS FOR SIMULATION

Battery Module	$V_{nominal}$ = 500V, Amp capacitor = 700Ah
UC Module	V_{rated} = 500V, Energy = 5.7kWh, $I_{nominal}$ = 2100A
Transformer 1	$P_{nominal}$ = 1MW, f_{rated} = 1kHz, N_1:N_2 = 1:2, L_1 = 10uH, L_2 = 20uH, R_1 = 0.01Ω, R_2 = 0.02Ω,
Transformer 2	$P_{nominal}$ = 100kW, f_{rated} = 10kHz, N_1:N_2 = 1:2, L_1 = 10uH, L_2 = 20uH, R_1 = 0.02Ω, R_2 = 0.04Ω,
Transformer 3	$P_{nominal}$ = 100kW, f_{rated} = 10kHz, N_1:N_2 = 1:1.67, L_1 = 3uH, L_2 = 5.5uH, R_1 = 0.02Ω, R_2 = 0.04Ω,
Inductors	L_{in1} = 100uH, L_{in2} = 500uH
Capacitors	C_{in} = 10mF, C_o = 20mF, C_{sn} = 0.15uF

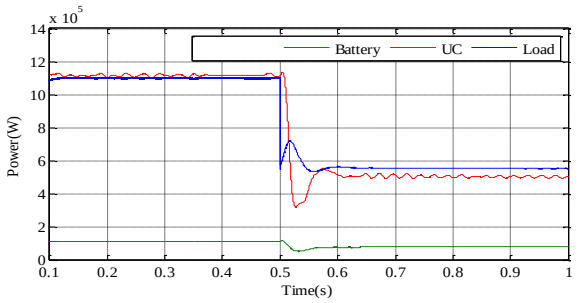

Fig. 11. Input and output power during battery/UC combined discharging mode

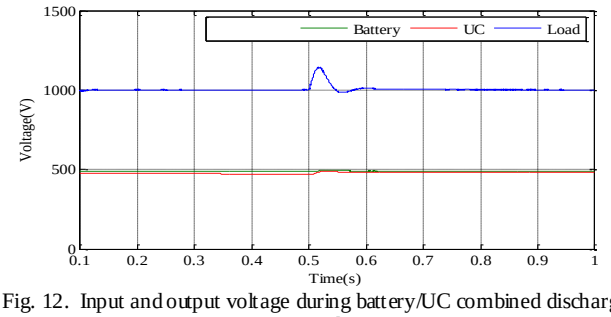

Fig. 12. Input and output voltage during battery/UC combined discharging mode

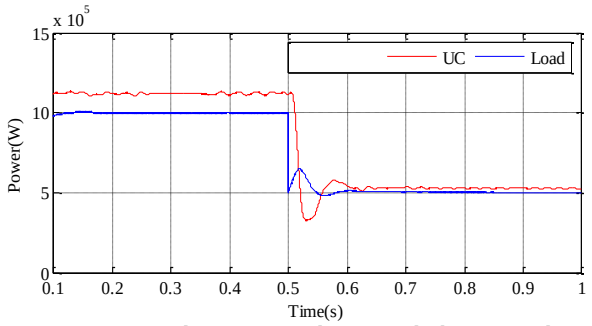

Fig. 13. Input and output power during UC discharging mode

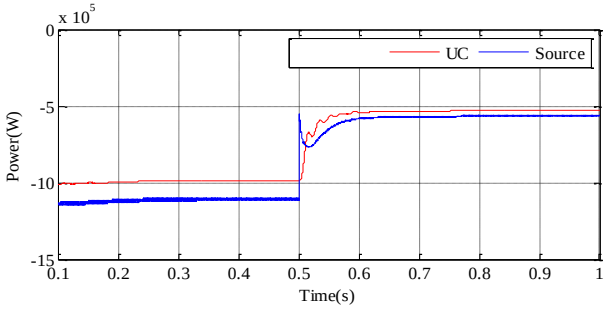

Fig. 14. Input and output power during UC charging mode

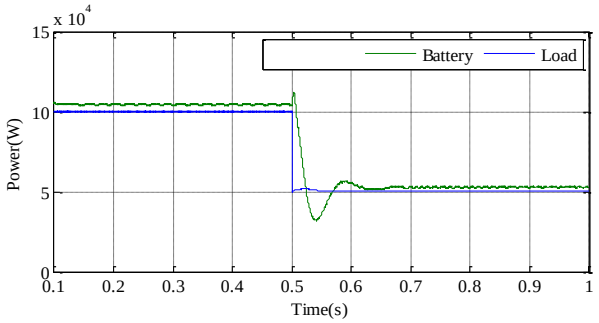

Fig. 15. Input and output power during battery discharging mode

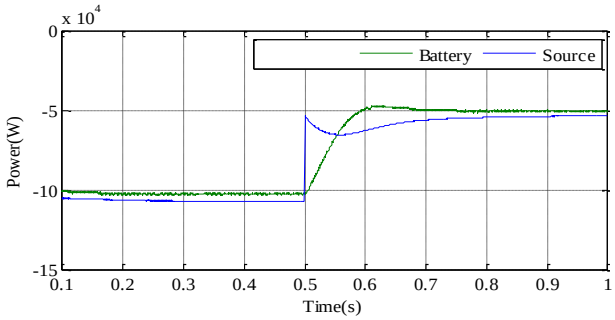

Fig. 16. Input and output power during battery charging mode

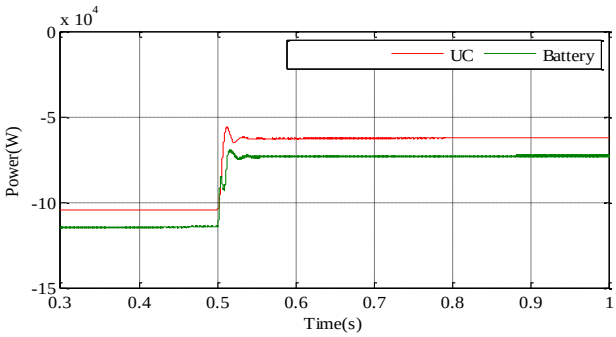

Fig. 17. Input and output power during battery/UC self-charging mode

VII. CONCLUSION

The feasibility of hybrid battery/ultracapacitor energy storage systems for naval applications has been explored in this manuscript and a new topology has been proposed. The BUCESS topology is designed to meet the requirements of both 100~500kW propulsion system and 1MW pulse power loads. The system consists of several isolated bidirectional dc-dc converters to implement charging and discharging of batteries and UCs. Dual active full bridge with IGBTs and GTOs is considered an excellent alternative for the BUCESS and phase-shift soft switching is utilized to control the power flow. The topology and parameters are provided and the results demonstrate the feasibility of the proposed BUCESS. The future research will focus on extending the operation time period of the system, minimizing the number of switching devices and studying the transient behavior of the system when the modes change or the modules are damaged.

VIII. REFERENCES

[1] S. McCluer, and J.F. Christin, "Comparing Data Center Batteries, Flywheels, and Ultracapactiors," American Power Conversion, White Paper #65, Rev. 1, 2008~2009.

[2] I. Porsche, H. Willis, and M. Ruszkowski, "Framework for Quantifying Uncertainty in Electric Ship Design," Santa Monica, CA: National Defense Research Institute, March 2004.

[3] F. Dupriez-Robin, L. Loron, F. Claveau, and P. Chevrel, "Design and Optimization of a Hybrid Sailboat by a Power Modeling Approach," in *Proc. IEEE Electric Ship Technologies Symposium*, April 2009, pp. 270-277.

[4] S. De Breucker, E. Peeters, and J. Driesen, "Possible Applications of Plug-in Hybrid Electric Ships," in *Proc. IEEE Electric Ship Technologies Symposium*, April 2009, pp. 310-317.

[5] G. Castles, A. Bendre and R. Pitsch, "Economic Benefits of Hybrid Drive Propulsion for Naval Ships," in *Proc. IEEE Electric Ship Technologies Symposium*, April 2009, pp. 515-520.

[6] S. Pay and Y. Baghzouz, "Effectiveness of Battery-Supercapacitor Combination in Electric Vehicles," in *Proc. IEEE Bologna PowerTech Conference*, June 2003, vol. 3.

[7] M. E. Baran and N. R. Mahajan, "DC Distribution for Industrial Systems: Opportunities and Challenges," in *Proc. IEEE Industrial and Commercial Power Systems Technical Conference*, May 2002, pp. 38-41.

[8] Y. Chung, W. Liu, M. Andrus, K. Schoder, S. Leng, D.A. Cartes, and M. Steurer, "Integration of a Bi-directional DC-DC Converter Model into a Large-scale System Simulation of a Shipboard MVDC Power System," in *Proc. IEEE Electric Ship Technologies Symposium*, April 2009, pp. 318-325.

[9] R.L. Steigerwald, R.W. De Doncker, and M.H. Kheraluwala, "A Comparison of High Power DC-to-DC Soft-Switched Converter Topologies," *IEEE Transactions on industry applications*, vol. 32, No. 5, pp. 1139-1145, Sept./Oct. 1996.

[10] H. Li, F.Z. Peng, J.S. Lawler, "A Natural ZVS Medium-power Bi-directional dc-dc Converter with Minimum Number of Devices," *IEEE Transactions on industry applications*, vol. 39, No. 2, Mar./Apr. 2003.

[11] J.M.Zhang, D.M.Xu, and Z. Qian, "An Improved Dual Active Bridge DC/DC Converter," in *Proc. of IEEE Power Electronics Specialists Conference*, 2001, pp. 232-236.

[12] F. Krismer, S. Round, J.W. Kolar, "Performance Optimization of a High Current Dual Active Bridge with a Wide Operating Voltage Range," in *Proc. of IEEE Power Electronics Specialists Conference*, 2006, pp. 1-7.

[13] M. Knauff, D. Niebur, and C. Nwankpa, "A Platform for the Testing and Validation of Dynamic Battery Models," in *Proc. IEEE Electric Ship Technologies Symposium*, April 2009, pp. 554-559.